The Effect of Increased Organic Solubility on Predicted CCN Activity in the Anthropogenically-Influenced Marine Boundary Layer

L.N. Hawkins,[1] et al.[2]

Aerosol particles in the marine boundary layer (MBL) are transported from their source region and processed in the atmosphere, and are therefore often mixtures of inorganic (*e.g.* SO_4^{2-}, NH_4^+, and NO_3^-) and organic components (*e.g.* carboxylic acid, hydroxyl, and saturated aliphatic functional groups). Although the solubility of inorganic aerosol components is fairly well known, the large number of unknown organic compounds present in ambient aerosol, in combination with their wide variety of hygroscopic properties, makes CCN activity of mixtures difficult to constrain. Here we present predicted CCN concentrations using recent measurements of submicron aerosol organic functional groups from the stratocumulus topped MBL in the southeast Pacific Ocean. The particles included both hydrophobic (saturated aliphatic C-CH) and hydrophilic (carboxylic acid COOH and hydroxyl COH) groups, in addition to small amounts of amine C-NH_2 and organosulfate $COSO_3$ groups. These measurements have been coupled with simultaneous measurements of particle size, inorganic elements, and inorganic ions to predict CCN activity of the ambient aerosol using a multi-component Köhler model. The model calculations show that CCN concentrations at 0.3% supersaturation are sensitive to the solubility of the organic fraction for the particle sizes observed during VOCALS-REx and that the sensitivity is inversely correlated with particle size below 180 nm. Above 180 nm, predicted CCN are close to 100% for all compositions. For the smallest particles, a 1% increase in average solubility resulted in a 6% increase in the fraction of activated particles. Predicted CCN concentrations in the region of highest continental influence (less than 600 km from shore) are highest and most sensitive to composition because of smaller particle size. The coastal region also has smaller effective cloud drop radii based on satellite observations from the Geostationary Operational Environmental Satellite (GOES-10) as expected in an area with elevated CCN.

[1]Scripps Institution of Oceanography, University of California, La Jolla, California, USA.

[2]This work was completed by Lelia Hawkins as part of SIO217D term projects created and advised by Lynn Russell, using measurements collected by D. Coffman, P. K. Quinn, D. S. Covert, and T. S. Bates and a model developed by G. Roberts. The submitted work has not yet been reviewed and approved by all of the coauthors and is not suitable for citation at this stage. Please contact Lelia Hawkins at lnhawkins@ucsd.edu to receive an update on these results.

0094-8276/09/$5.00

1. Introduction

The extent to which aerosols impact cloud optical properties, lifetime, and precipitation patterns by acting as cloud condensation nuclei (CCN) is controlled by their ability to grow in a saturated air parcel (hygroscopic growth), which in turn is controlled by their size and chemical composition [Köhler,1936; Roberts et al., 2002; Quinn et al., 2007]. In conditions with high supersaturations or for particles of uniform composition, particle size may be more critical for predicting accurate CCN concentrations [Dusek et al., 2006; Hawkins et al., 2008]. For low supersaturations, when composition varies with size, or when particles are small, both particle size and composition are relevant [Nenes et al., 2002; Roberts et al., 2002]. Organic components in ambient aerosol range from insoluble (hydrocarbons) to soluble (acids) [Russell et al., 2009; Gilardoni et al., 2007; Maria et al., 2002, 2003] in varying proportions but are often treated as insoluble in CCN studies due to insufficient chemically specific measurements to constrain estimates of solubility. However, the presence of organic compounds can drastically reduce or increase CCN concentrations by lowering solubility, increasing molecular weight, and suppressing surface tension [Ervens et al., 2005; Chan et al., 2008]. Fourier Transform Infrared (FTIR) spectroscopy permits us to constrain solubility of the organic mass based on functional group contribution to total organic mass (OM).

The southeast Pacific ocean is dominated by marine stratocumulus clouds, which generally have low supersaturations (around 0.3%) [Martin et al., 1994]. Typically the marine atmosphere also has low background particle concentrations [O'Dowd and de Leeuw, 2007; Hawkins et al., 2008]. Because of this, marine stratocumulus clouds are sensitive to additional CCN [Albrecht, 1989] such that even small perturbations to the existing concentration of CCN may have a significant impact on cloud reflectivity and lifetime.

The specific conditions for which particle composition and organic solubility are relevant will vary with the chemical and physical properties of the aerosol and with supersaturation and cannot be strictly defined. For this reason, thermodynamic models are needed to understand how or if small scale changes in size and composition affect CCN concentration. Here we use a multi-component Köhler model described by Roberts et al. [2002] to investigate the importance of constraining organic composition with functional group fraction on predicted CCN concentrations for the range of observed particle concentrations and chemical compositions in the low supersaturation (SS) environment of the southeast Pacific marine boundary layer.

2. Methods

2.1. Sample Collection

Submicron particles were measured at 5-minute intervals by an Aerodyne Quadrupole Aerosol Mass Spectrometer (Q-AMS) through an isokinetic sampling inlet located on the

forward deck of the R/V Ronald H. Brown approximately 18 m above sea level [Quinn et al., 2007; Bates et al., 2008]. The sample line was partitioned to collect particles on filters located downstream of a 1 μm sharp-cut cyclone (SCC 2.229 PM1, BGI Inc.) in a temperature and humidity controlled enclosure. Samples were collected on 37 mm teflon filters (Pall Inc.) over 12 to 24 hours (short samples) with simultaneous 24 hour (duplicate and long samples) for offline FTIR spectroscopic and X-ray Fluorescence (XRF) analyses. Particle size distributions were measured with a Differential Mobility Particle Sizer (DMPS) from the shared sampling inlet.

2.2. Fourier Transform Infrared Spectrosocpy (FTIR) and X-Ray Fluorescence (XRF)

FTIR samples were kept at 0^{o}C prior to FTIR spectroscopic analysis to reduce evaporative losses of organic compounds and to reduce artifacts from condensed-phase chemical reactions. Infrared absorbance spectra of each sample and blank filter were measured non-destructively using a Bruker Tensor 27 spectrometer with RT-DLATGS detector [Gilardoni et al., 2007] and were interpreted using a revised algorithm [Russell et al., 2009] and calibration standards [Gilardoni et al., 2007; Maria et al. 2002; 2003; Maria and Russell, 2005]. Quantified organic functional groups include saturated aliphatic C-CH (alkane), non-acidic hydroxyl C-OH (alcohol), primary amine C-NH_2, carboxylic acid COOH, and organosulfate $COSO_3$ groups. Non-acidic carbonyl C=O, aromatic C=C-H, and unsaturated aliphatic C=C-H (alkene) groups were below detection limit in all samples and were not included in this analysis. X-ray fluorescence on the teflon filters was completed by Chester Labnet (Tigard, Oregon) and provided concentrations of elements heavier than neon [Maria et al., 2003; Gilardoni et al., 2007; Russell et al., 2009].

2.3. Quadrupole Aerosol Mass Spectrometry

The Aerodyne Quadrupole Aerosol Mass Spectrometer (Q-AMS) measures bulk non-refractory submicron aerosol chemistry and component-specific size distributions in real-time at 5-minute resolution [Jimenez 2003, Jayne 2000]. The instrument comprises a Time-of-Flight (ToF) sizing inlet followed by a 600^{o}C vaporizer and electron impact ionizer. From there the sample is analyzed using a quadrupole mass spectrometer with 1 amu resolution. Quantified components include $SO_4{}^{2-}$, $NO_3{}^-$, $NH_4{}^+$, and organics.

2.4. Multi-Component Köhler Model for Calculating CCN at 0.3% SS

The Köhler equation [Seinfeld and Pandis, 2006] (Eq. 1) relates particle size and composition to the supersaturation at which droplet nucleation is thermodynamically favorable and consists of the Kelvin term, which accounts for the increased equilibrium vapor pressure over a curved surface relative to a flat plane, and the Raoult term, which accounts for the decreased equilibrium vapor pressure over salt solutions relative to pure water:

$$ln(\frac{p_w(D_p)}{p_o}) = \frac{4M_w\sigma_w}{RT\rho_w D_p} - \frac{6n_s M_w}{\pi\rho_w D_p^3} \quad (1)$$

where ρ_w and ρ_o are the densities of pure water and the relevant solution, D_p is the particle diameter, M_w is the molecular weight of water, σ is the surface tension of the solution, and n_s is the number of moles of solute. Using the general form of the Köhler equation it is not trivial to include multiple solutes, especially those with widely varying solubilities and surface tensions. For this application, a modified Köhler equation is necessary.

Predicted CCN are calculated using a multi-component Köhler model [Roberts et al. 2002] for three case studies: (1) a 1-component NH_4HSO_4 only model, (2) a 3-component

Table 1. Predicted CCN (cm^{-3}) and activated fraction in each of the three cases for the 21 samples, in order of increasing distance from the coast.

Composition	Case 1 NH_4HSO_4		Case 2 NH_4HSO_4, Dust, and Insol. Organic		Case 3 NH_4HSO_4, Dust, Slightly sol. and Insol. Organic	
Distance (km)	CCN	CCN/CN	CCN	CCN/CN	CCN	CCN/CN
171	445	0.94	419	0.89	431	0.91
221	360	0.93	336	0.87	342	0.88
244	274	0.86	226	0.71	240	0.75
350	231	0.94	213	0.87	217	0.88
386	133	0.98	129	0.95	131	0.97
387	179	0.96	170	0.91	173	0.92
391	447	0.92	402	0.83	420	0.87
392	237	1.00	234	0.98	235	0.99
423	237	0.97	229	0.94	231	0.95
425	119	0.96	113	0.92	116	0.94
425	206	0.93	191	0.86	195	0.88
453	116	0.97	111	0.92	114	0.94
500	203	0.95	193	0.90	195	0.91
575	170	0.95	157	0.88	162	0.91
670	150	0.98	145	0.95	146	0.95
701	116	0.96	111	0.92	114	0.94
704	123	0.97	118	0.93	120	0.95
890	101	0.97	97	0.93	98	0.94
1061	85	0.97	81	0.92	83	0.94
1088	49	0.95	45	0.89	47	0.91
1162	65	0.88	54	0.74	58	0.78

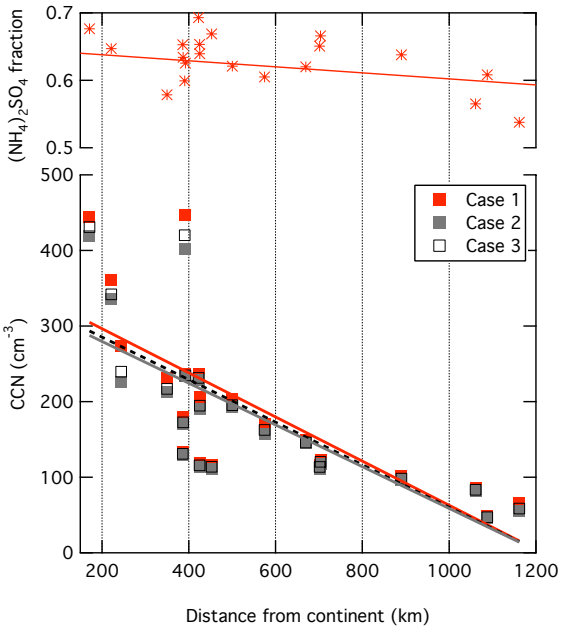

Figure 1. (a) Fraction of NH_4HSO_4 (Cases 2 and 3 only) and mean particle diameter compared with distance from the continent. (b) Predicted CCN concentration compared with distance from the continent.

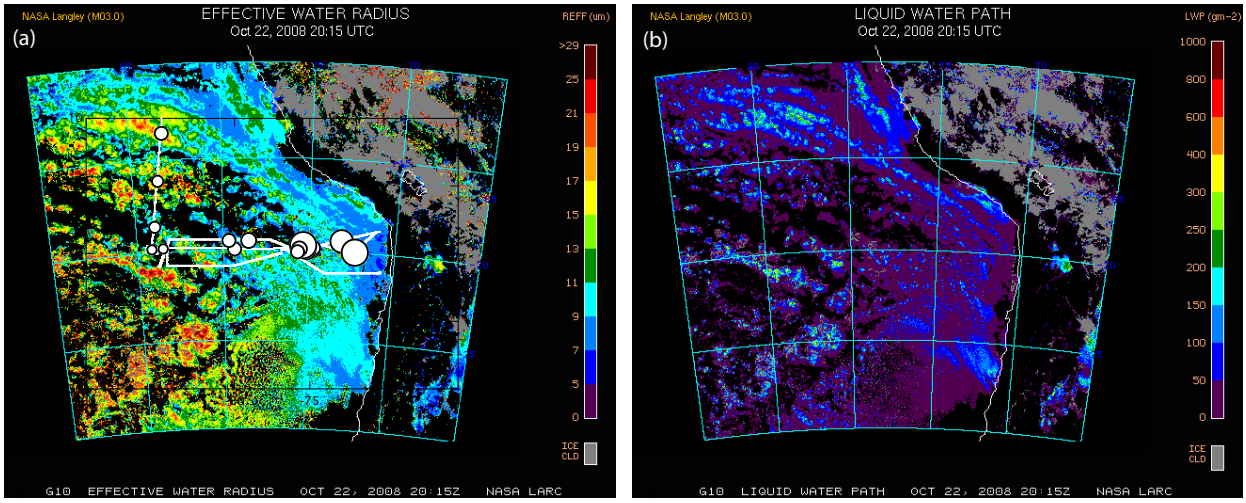

Figure 2. Images from the GOES-10 satellite showing (a) effective water radius (μm) and (b) liquid water path (g m^{-2} for 22 October 2008. The ship track and average location of filter samples are overlaid on the map of effective water radius to illustrate the qualitative relationship between CCN concentration (marker size) and droplet radius since droplet number concentrations are not available at this time [http : //catalog.eol.ucar.edu/cgi − bin/vocals/imagewrap.nonav?file$_u$rl = /vocals/ops/goes − 10/20081022].

model including NH_4HSO_4, insoluble organics, and insoluble inorganics (dust), and (3) a 4-component model including NH_4HSO_4, insoluble organics, dust, and slightly soluble organics. AMS NH_4^+ and SO_4^{2-} were present at approximately a 1:1 molar ratio are treated as NH_4HSO_4 in all three cases for simplicity. AMS NO_3^- was very low and is not included in this analysis. Elemental components from sea salt (Na, Cl) were below detection limit in greater than 80% of the samples. Elements above detection limit in greater than 20% of samples include Sn, V, Fe, K, Br, Ca, Al, Cr, and Ni; these elements are treated as "dust" (completely insoluble) in the second and third model calculations for simplicity. This assumption is not likely to affect the model prediction given that the elements make up between 1% and 6% of the submicron particulate mass (PM_1). The organic fraction (from FTIR spectroscopy) is treated as "insoluble organic" in Case 2, then partitioned by functional group into two categories for Case 3. Alkane and amine groups are treated as "insoluble organic"; acid, alcohol, and organosulfate groups are treated as "soluble organic" (using the solubility of adipic acid, 0.06 g ml^{-1} water). The measured organic mass was approximately evenly split between soluble and insoluble groups. The DMPS size distributions were used to determine appropriate model inputs (geometric mean diameter, geometric standard deviation, and number concentration) for particles above 80 nm. Some periods were characterized by bimodal number distributions with a significant number fraction of total particles below 80 nm. Only the larger mode was included in the model input due to the model limitation of unimodal particle distribution and the low fraction of even completely soluble particles activating below 80 nm at 0.3% supersaturation. CCN concentrations are compared for the 3 conditions at 0.3% SS, in the range of (estimated) SS of southeast Pacific marine stratocumulus (0.2% to 0.4%) [Hoppel et al., 1996; Tomlinson et al., 2007] and the SS of collated CCN measurements.

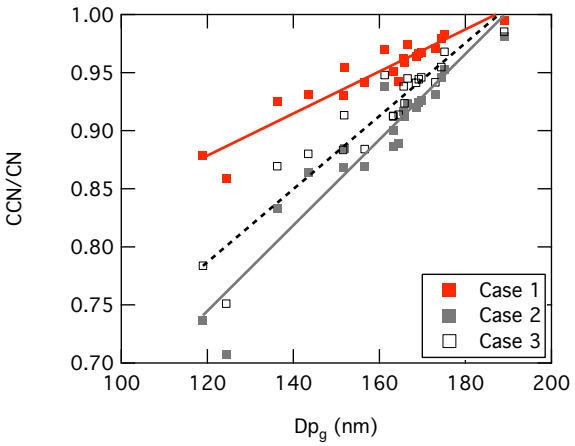

Figure 3. Predicted activated fraction (CCN/CN) compared with geometric mean diameter (Dpg) for all three cases.

3. Predicted CCN concentrations for 3 Compositions at 0.3% SS

Table 1 shows the predicted CCN concentrations and activated fractions (CCN/CN) for each of the three cases ordered by distance from the coast. For the 1-component model (Case 1) that assumes 100% NH_4HSO_4, most samples were predicted to have over 90% of the particles activate at 0.3% SS. For the 3-component model (Case 2) that assumes all organics are insoluble, some samples have as low as 71% of the particles activating, which corresponds to a maximum drop in CCN from Case 1 of about 50 cm^{-3}. For the 4-component model (Case 3) that separates the organic fraction into slightly soluble and insoluble, the activated fractions are slightly higher than those of Case 2 but still significantly lower than those of Case 1.

Figure 1 shows the dependence of CCN concentration on distance from the coast. The small change in predicted CCN

number between the 3 cases indicates that decrease in total particle concentration (through dilution) is driving the geographic distribution of CCN, though the absolute number of CCN at each location is sensitive to particle chemistry (Table 1). Figure 2 shows the spatial distribution of CCN for Case 3 in relation to satellite images of cloud drop effective radius and liquid water path and is discussed further in the next section. Figure 3 shows the dependence of activated fraction on mean particle size. The model calculations show that particle size is most important when the fraction of soluble material is lowest, as indicated by the steeper slope for Case 2. For sizes above 180 nm, the particle composition does not have a significant impact on predicted CCN.

4. Discussion

At the smallest observed mean diameter (120 nm), including the organic fraction as completely insoluble lowers the predicted CCN by over 10% relative to a completely soluble particle. The fraction of soluble inorganic mass in the second case was approximately 50% and ranged from 41% to 67%; this is a large change in composition between Cases 1 and 2 and is the main cause of the observed change in activated fraction between the two cases. The effect of chemical composition among the three cases is most notable for particles below 160 nm. Because the mean diameter is below 160 nm only for particles less than 600 km away from the continent, the effect of chemistry is also most notable in the samples collected near shore (Fig. 1). Farther from shore, the particles are larger due to increased time for cloud processing and condensation of semi-volatile compounds. Above approximately 160 nm, treating the oxidized organic groups as soluble organic compounds does not produce a significant difference in predicted CCN concentration. For all samples, including soluble organics lowers the predicted CCN at least a few percent though this is likely to be within the uncertainty associated with variability in ambient organic surface tension and molecular weight. Accounting for these effects is beyond the scope of the current study but the expected result would be added variability in the predicted CCN concentration, especially close the continent where organic mass concentrations are higher. Above 55% percent soluble material, there is no observable change in activated fraction with increasing soluble fraction indicating a threshold for chemical influence on CCN applies to all three cases.

The Geostationary Operational Environmental Satellite (GOES-10) satellite shows effective cloud drop radius (R_{eff}) and liquid water path (LWP, Fig. 2) for 22 October 2008, approximately half-way into the VOCALS-REx sampling period. We have overlaid the ship track, average filter location, and predicted CCN from Case 3 as a guide for the eye. Consistent with predicted CCN concentrations and the Twomey effect [Twomey, 1977], drops are smaller (approx. 10 μm) near the coast, where CCN concentrations are highest. At the farthest sampling site (-85°W), effective cloud drop radii are approximately 20 μm. Drop number concentrations are not directly available but the observed constant value for LWP (with increasing distance from the continent) can be used to infer an increase in cloud droplet number accompanying the decrease in droplet radius.

5. Conclusion

Predicted CCN concentrations in the southeast Pacific were found to be sensitive to organic composition and solubility for particles below 160 nm diameter. This is relevant in the region within 600 km of Peru and Chile where particle concentrations are highest and particles are smaller due to limited time for atmospheric processing, indicating that future changes in anthropogenic outflow may be important for coastal cloud optical properties. In these conditions, the number of predicted CCN dropped by as much as 10% when a more constrained solubility was assigned to the organic functional groups. Observations by the GOES-10 satellite of cloud drop effective radius and liquid water path are consistent with the geographic distribution predicted here from chemical and physical measurements of submicron aerosol particles. These results are specific to the supersaturations, particle size, number, and chemistry of the southeast Pacific MBL.

Acknowledgments. We would like to thank Lynn Russell, Doug Day, and anonymous reviewers for technical and writing help.

References

Albrecht, B.A. 1989, *Science*, 245, 4923, 1227-1230.

Bates, T.S. et al., 2008, *J. Geophys. Res*, 113.

Chan, M.N. , S. M. Kreidenweis, and C. K. Chan, 2008, *Environ. Sci. Technol.*, 42 (10), 3602-3608, doi: 10.1021/es7023252.

Dusek, U., et al., 2006, *Science*, 312, 5778, 1375-1378.

Ervens, B., G. Feingold, and S. M. Kreidenweis, 2005, *J. Geophys. Res.*, 110, doi:10.1029/2004JD005634.concentration,

Gilardoni, S., et al., 2007, *J. Geophys. Res.*, 112, doi:10.1029/2006JD007737.

Hawkins, L. N., L. M. Russell, C. H. Twohy, and J. R. Anderson, 2008, *J. Geophys. Res.*, 113, doi:10.1029/2007JD009150.

Hoppel, W. A., G. M. Frick, and J. W. Fitzgerald, 1996, *J. Geophys. Res.*, 101, 26,553 26,565.

Jayne, J. T., D. C. Leard, X. Zhang, P. Davidovits, K. A. Smith, C. E. Kolb, and D. R. Worsnop, 2000, *Aerosol Sci. Technol.*, 33(1 2), 4970.

Jimenez, J. L., et al., 2003, *J. Geophys. Res.*, 108(D7), 8425, doi:10.1029/2001JD001213.

Köhler, H., 1936, *Transactions of the Faraday Society*, 32, 1152–1161.

O'Dowd, C.D. and G. de Leeuw, 2007, *Phil. Trans. Royal Soc.*, 365(1865), 1753.

Maria, S. F., L. M. Russell, B. J. Turpin, and R. J. Porcja, 2002, *Atmos. Env.*, 36, 5815-5196.

Maria, S. F., et al., 2003, *J. Geophys. Res*, 108(D23), doi:10.1029/2003JD003703.

Maria, S. F. and L. M. Russell, 2005, *Env. Sci. Tech*, 39(13), 4793-4800.

Nenes, A. and Charlson, R.J. and Facchini, M.C. and Kulmala, M. and Laaksonen, A. and Seinfeld, J.H., 2002, *Geophys. Res. Lett.*, 29(17), 29-31.

Quinn, P.K., T. S. Bates, D. J. Coffman, and D. S. Covert, 2007, *Atmos. Chem. Phys. Discuss.*, 7, 1417114208.

Roberts, G. C., P. Artaxo, J. Zhou, E. Swietlicki, and M. O. Andreae, 2002, *J. Geophys. Res.*, 107(D20), 8070, doi:10.1029/2001JD000583.

Russell, L. M., et al., 2009, *J. Geophys. Res., in press*

Seinfeld, J. H., and S. N. Pandis, 1998, *Atmospheric Chemistry and Physics: From Air Pollution to Climate Change*, 1326, John Wiley, New York.

Tomlinson, J.M., R. Li, and D. R. Collins, 2007, *J. Geophys. Res.*, 112, doi:10.1029/2006JD007771.

Twomey, S., 1977, *J. Atmos. Sci.*, 34(7) 1149-1152.